(1)

Ibn Al-Haitham Journal for Pure and Applied Sciences

Journal homepage: jih.uobaghdad.edu.iq PISSN: 1609-4042, EISSN: 2521-3407 IHJPAS. 2025, 38(4)



Calculation of Semi-Major and Semi-Minor Radii and Deformation Parameters for Molybdenum $^{86-100}_{-42}Mo$ Isotopes

Reem Gani Abdulrazzaq Mohammed ^{1*} → Sameera Ahmed Ebrahiem → and Mustafa H. Shareef →

^{1,2}Department of Physics, College of Education for Science (Ibn-AL-Haitham), University of Baghdad, Baghdad, Iraq

³Department of Physics, Faculty of Science, Karabuk University, Karabuk, 78050, Türkiye. *Corresponding Author.

Received: 4 May 2025 Accepted: 24 July 2025 Published: 20 October 2025

doi.org/10.30526/38.4.4165

Abstract

This study explores the nuclear properties of even-numbered molybdenum ($^{86-100}_{42}Mo$) isotopes in the mass range 86 to 100. It focuses on the calculations of fundamental nuclear properties such as distortion coefficients (β_2 and δ), electric quadrupole moments (Q_0), root-mean-square charge radii, and reduced transition probabilities B(E2)↑. These calculations were derived using a theoretical framework based on the distorted shell model and implemented in MATLAB. The evaluation also included the identification of the two quasi-nuclear shape axes (major and minor), from which three-dimensional representations of the isotopic shapes were generated. The analysis revealed a gradual decrease in distortion coefficients and transition probabilities with increasing mass number, indicating a trend toward nuclear stability. We observed a significant decrease in distortion near the magic number of neutrons, demonstrating the enhanced stability resulting from closed shells. The results are in good agreement with theoretical predictions and experimental data, providing a deeper understanding of the behavior of molybdenum isotopes and contributing to the expansion of knowledge of nuclear shape evolution, charge distribution, and nuclear transitions in intermediate-mass nuclei.

Keywords: Electric quadrupole moments, Possibility of electrical transition, Half-life mean-squared, Charge distribution, Radius $\langle r^2 \rangle$, Transition probability B (E2;0⁺ \rightarrow 2⁺) \uparrow .

1.Introduction

A nucleus always maintains its spherical shape when it contains a certain number of nucleons, known as magic numbers (2, 8, 20, 28, 50, 82, and 126) (1,2). However, when the total number of protons and neutrons deviates from these values, the nucleus tends to lose its spherical symmetry and become distorted (3-5). Nuclei with magic numbers exhibit greater stability due to their closed shell configuration⁵. Nuclear distortion is due to the spatial distribution of valence nucleons within incomplete shells, meaning that this distortion most often occurs when both the proton (Z) and neutron (N) shells are incomplete (6).

The most common type of nuclear distortion is the quadrupole distortion, where the nucleus assumes an elongated (ellipsoidal) or flattened (compact) shape. In even-even nuclei, the first

excited energy state is typically the 2^+ state, and the transition from this state to the 0^+ ground state provides a profound understanding of the nucleus's structure. Electromagnetic transitions, especially the electromagnetic quadrupole (E2) transitions, are essential tools for exploring these properties (7). The low electromagnetic transition probability, B (E2; $0^+ \rightarrow 2^+$), provides essential information about the nucleus's structure, especially for low-energy excitations. High values of B(E2) indicate a significant tetragonal distortion in the nucleus, reflecting collective behavior within these systems(8).

Determining the tetragonal intrinsic moment (Q_o) requires an accurate measurement of the electromagnetic quadrupole transitions between the ground state and the excited state(9). This parameter is essential for exploring shape transitions and allows predictions of different properties of even-even nuclei based on the extent of their distortion. Understanding nuclear deformation is fundamental to characterizing shapes such as elongated and compact. Ultimately, the tetrahedra self-moment is a quantitative measure of the nuclear charge distribution and provides insights into deviations from spherical symmetry(10).

2. Materials and Methods

Nuclear deformation arises from the arrangement of valence nucleons within the unfilled nuclear shells. Distortion occurs only when both proton P and neutron n shells are not completely filled. One fundamental type of nuclear deformation is quadrupole distortion (11), where the nucleus may adopt either a prolate (elongated) or oblate (flattened) shape(12), as illustrated in the accompanying **Figure 1** (13).

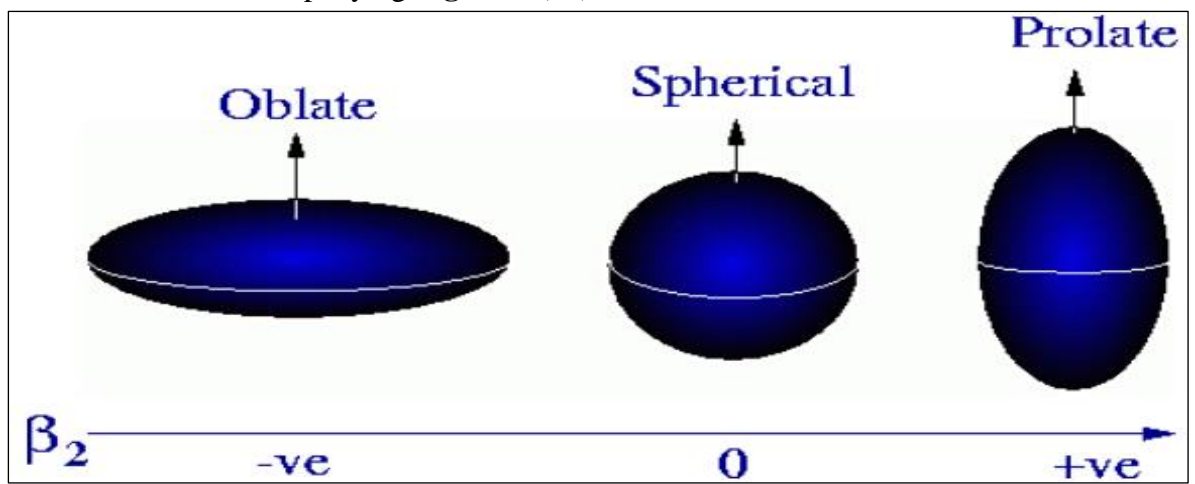


Figure .1. A diagram with flattened, stretched shapes and spherical. Arrows on the flattened and stretched shapes indicate symmetry (14, 15).

Their liquid drop model of the nucleus supple and soft, thus permitting them to detect considerable distortions in its shape from a perfect sphere ¹⁶. Anywhere the number of neutron (N) had a high frequency (6), a considerable number of nuclei were identified (N) and protons (P) is markedly distant from the magnetic values, exhibiting a distorted charge distribution (17).

The distortion parameter β_2 is a model based on quantum mechanics(18). Considering that these probabilities describe the interactions of nucleons with all other nucleons in all remainder nucleons in the nucleus:

$$\beta_2 = 4\pi / 3ZR_o^2 \left[B(E2) \uparrow e^2 b^2 / e^2 b^2 \right]^{1/2} \tag{1}$$

Where
$$R_o = 0.0144 A^{1/3}$$
 (2)

And
$$B(E2) \uparrow = 2.6E_{\gamma}^{-1}Z^2A^{-2\backslash 3}$$
 (3)

In this context, A denotes the mass number of a nucleus (19), Z represents the atomic number, and $E\gamma$ signifies the gamma-ray transitions energy, measured in kiloelectronvolts (KeV).

To calculate the deformation parameter δ , we rely on the internal electric quadrupole Q_o because it provides information on deformation and shape, measuring the distortion and spherical symmetry of the charge distribution. The quadrilateral deformation coefficient (the degree of variation in the spherical shape) can be calculated using the quadrilateral moments $Q_o(20,21)$

$$\delta = 0.75 Q_o / (\langle r^2 \rangle Z) \tag{4}$$

Where
$$Q_o = [(16 \pi / 5) B(E2)e^2 b^2 / e^2]^{\frac{1}{2}}$$
 (5)

The average radius < r2 > can be calculated:

$$< r^2 > = 0.63 R_0^2 (1 + 10/3 (\pi a_0/R_0)^2) / (1 + (\pi a_0/R_0)^2) (\dot{A} \le 100)$$
 (6)

Whence the Ro: radial Woods-Saxon parameters are, Ro=1.07A^{1/3} fm and ao=0.55(fm), with ao from fast electron scattering information (22).

In general, shapes of nuclei are approximately spherical when a nucleus is stable, since it lowers the surface energy of the nucleus (23). Hence, small sections of spheres are seen (24,25), as with the region 150<A<190

$$\boldsymbol{\delta} = \Delta \boldsymbol{R} / \boldsymbol{R} \tag{7}$$

Whêre:

 ΔR denotes the difference between the semi-major and semi-minor axes (9,26).

While the average of the nuclear radius represents by R, due to, as assumed (27),

$$\Delta \mathbf{R} = (\mathbf{b} - \mathbf{a}) \tag{8}$$

The subsequent equations provide the semi-axes (a) and (b)(28).

$$a = \sqrt{\langle r2 \rangle (1.66 - \frac{2\delta}{0.9})}$$
 (9)

$$b = \sqrt{5} < r2 > -2a^2 \tag{10}$$

3. Results

This study focused on the nuclear properties of the element molybdenum (Mo), a transition metal with atomic number 42. Known for its silver appearance and high resistance to heat and corrosion, molybdenum is widely used in steel alloys to enhance their strength and thermal durability. Some of its isotopes are also employed in nuclear structure studies due to their unique properties.

The analysis covered molybdenum isotopes with mass numbers ranging from 80 to 100 Several nuclear indicators were calculated, including electric transition probabilities, deformation parameters, and electric quadrupole moments (Q_0), using gamma energy values taken from Firestone (29).

The results indicated a gradual decrease in deformation parameter values from 0.2276 to 0.2008 as the mass number increased, with an exception at the heaviest isotope. These values were generally consistent with theoretical calculations from the Global, as shown in **Figures 2** and **3**. Similarly, the electric transition probabilities, calculated using **Equation 3**, decreased from 0.4144e²b² to 0.3975e²b² with increasing mass number, and were in good agreement with experimental values (**Table 1**).

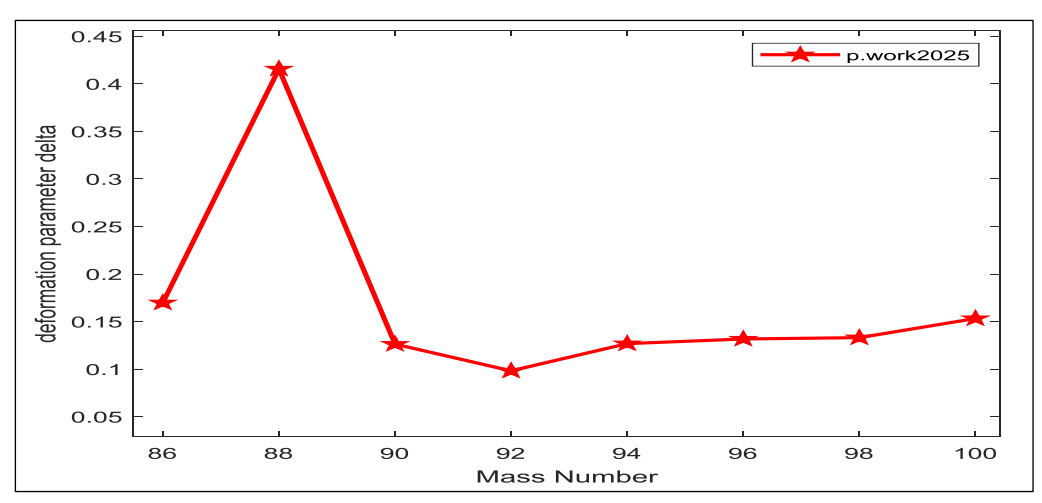


Figure 2. The shows the relationship between the mass number of the element Mo and the distortion coefficient delta.

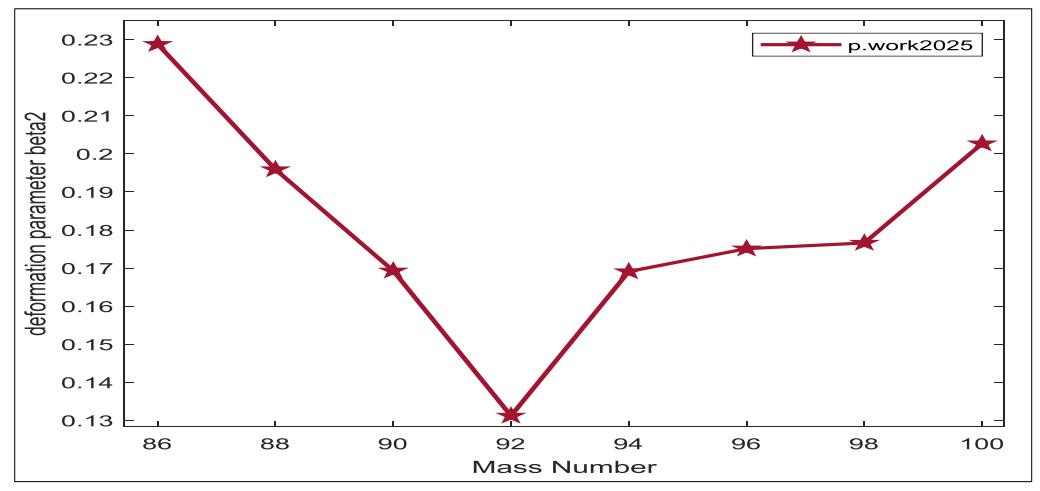


Figure 3. The shows the relationship between the mass number of the element Mo and the beta distortion fatcter.

Table 1. Quadripole moment Tetrapolar electrode (Q_0) in barns, gamma energy to the first level E_{γ} , low electrostatic transition potential B(E2) \uparrow in e^2 b^2 units, average nuclear radius (R_0^2), number of neutrons (N), mass numbers of isotopes (A) molybdenum and parameters of deformation (β_2 , δ) for molybdenum Mo.

	N	E_{γ}	The Theore	A present Work					
A			$B(E_2)$ $\uparrow (e^2b^2) for$ Global Best Fit (29)	eta_2 for Global Best Fit	δ	$oldsymbol{eta}_2$	$oldsymbol{Q}_{^{\circ}}\left(oldsymbol{b} ight)$	$B(E_2)$ $\uparrow (e^2b^2)$	R ²
86	44	568	0.41	0.2276	0.1698	0.2288	2.0412	0.4144	28.06
88	46	740.53	0.31	0.1949	0.4157	0.1959	1.7740	0.3130	28.49
90	48	947.97	0.238	0.1682	0.1263	0.1693	1.5562	0.2409	28.92
92	50	1509.49	0.147	0.1303	0.0982	0.1312	1.2243	0.1491	29.35
94	52	871.096	0.251	0.1678	0.1268	0.1691	1.6001	0.2547	29.77
96	54	778.245	0.277	0.1739	0.1317	0.1751	1.6810	0.2811	30.19
98	56	734.75	0.270	0.1693	0.1331	0.1766	1.7182	0.2937	30.61
100	58	535.57	0.39	0.2008	0.1532	0.2027	1.9990	0.3975	31.02

Deformation factors based on quadrupole moments also showed a decreasing trend. However, for the isotope with mass number 50 a magic number the deformation value was significantly lower, indicating a high level of nuclear stability.

The electric quadrupole moments, measured in barns, ranged from a maximum value of $2.0412e^2b^2$ to a minimum of $1.5562e^2b^2$, as illustrated in **Figures 4** and **5**.

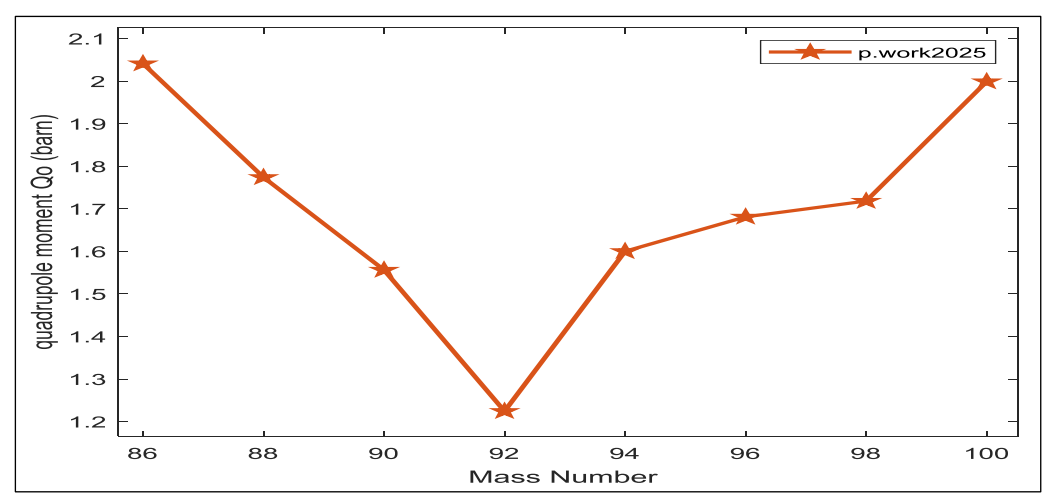


Figure 4. The shows the relationship between the mass number of the element Mo and the electric quadrupole moment.

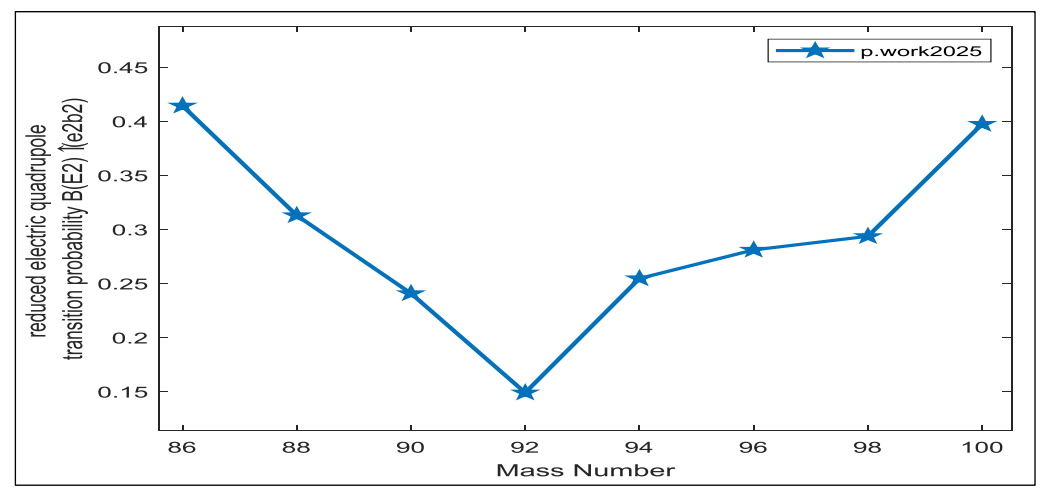


Figure 5. The shows the relationship between the mass number of the element Mo and the probability of the central quadrupole transition.

Further analysis using the even-even isotopes of molybdenum involved calculating transition probabilities and half-life values based on gamma energy and half-life data. These ranged from (0.0354 to 2.1975*10⁻²⁷) seconds for mean-lives and from (28.2828 to 4.5506*10²⁶) for transition probabilities, as summarized in **Table 2**.

Table 2. Average half-life t (s) for molybdenum (Mo) isotopes, neutron numbers N, gamma energy to the first state, probability T of transition, and A represent mass numbers.

	A	N	$E_i(Kev)$	$E_2(Kev)$	$\frac{t_t(s)}{2}$	T(s)	$\tau(s)$
42	86	44	568	568	19.6 s	28.2828	0.0354
	88	46	740.53	740	(8.0m) 480	692.6407	0.0014
	90	48	947.97	947	(5.56 h)20.016	28.8831	0.0346
	92	50	1509.49	1509	$(0.35 \text{ ps})0.35*10^{-12}$	$5.0505*10^{-13}$	$1.9800*10^{12}$
	94	52	871.096	871	(2.88 ps)2.88*10 ⁻¹²	$4.1558*10^{-12}$	$2.4062*10^{11}$
	96	54	778.245	778	(3.66 ps)3.66*10 ⁻¹²	$5.2814*10^{-12}$	$1.8934*10^{11}$
	98	56	734.75	734	(21.8 ns)21.8*10 ⁻⁹	$3.1457*10^{-8}$	$3.1789*10^7$
	100	58	535.57	535	$(1.00*10^{19} \text{ y})$ $3.1536*10^{26}$	4.5506*10 ²⁶	2.1975*10 ⁻²⁷

In **Table 3**, the semi-major and semi-minor axes (a, b) were calculated using **Equations 9** and (10), while their difference was obtained from **Equation 8**. The root mean square charge radius was calculated using **Equation 6**. These values showed a direct correlation with

increasing mass number, and were generally close to experimental data from the source, as depicted in **Figure 6**.

Table 3. Additionally, it includes the mass numbers (A), the major and minor axes (b, a), neutron counts (N), the root mean square of the radius $< r^2 >^{(1/2)}$, as well as their separation (ΔR) for the isotopes of molybdenum, described in two distinct ways.

	A	N	A Theoretical Values	A present Work							
			$ \langle r^2 \rangle^{\frac{1}{2}} $ fm $ (30) $	$\langle r^2 angle fm$	$\langle r^2 angle^{rac{1}{2}}$ fm	a (fm)	b (fm)	ΔR_1	ΔR_2	ΔR_3	
42	86	44		21.4702	4.6335	2.4443	3.3494	0.8018	0.9052	1.1469	
	88	46		21.7386	4.6624	2.50222	3.2849	0.6936	0.7827	0.9892	
	90	48	4.3265	22.0047	4.6909	2.5498	3.2328	0.6056	0.6830	0.8613	
	92	50	4.3151	22.2686	4.7189	2.6145	3.1502	0.4742	0.5358	0.6726	
	94	52	4.3529	22.5304	4.7466	2.5639	3.2537	0.6170	0.6898	0.8728	
	96	54	4.3847	22.7901	4.7738	2.5611	3.2789	0.6453	0.7178	0.9105	
	98	56	4.4091	23.0479	4.8008	2.5654	3.2927	0.6567	0.7273	0.9243	
	100	58	4.4468	23.3038	4.8274	2.5303	3.3663	0.7608	0.8360	1.0681	

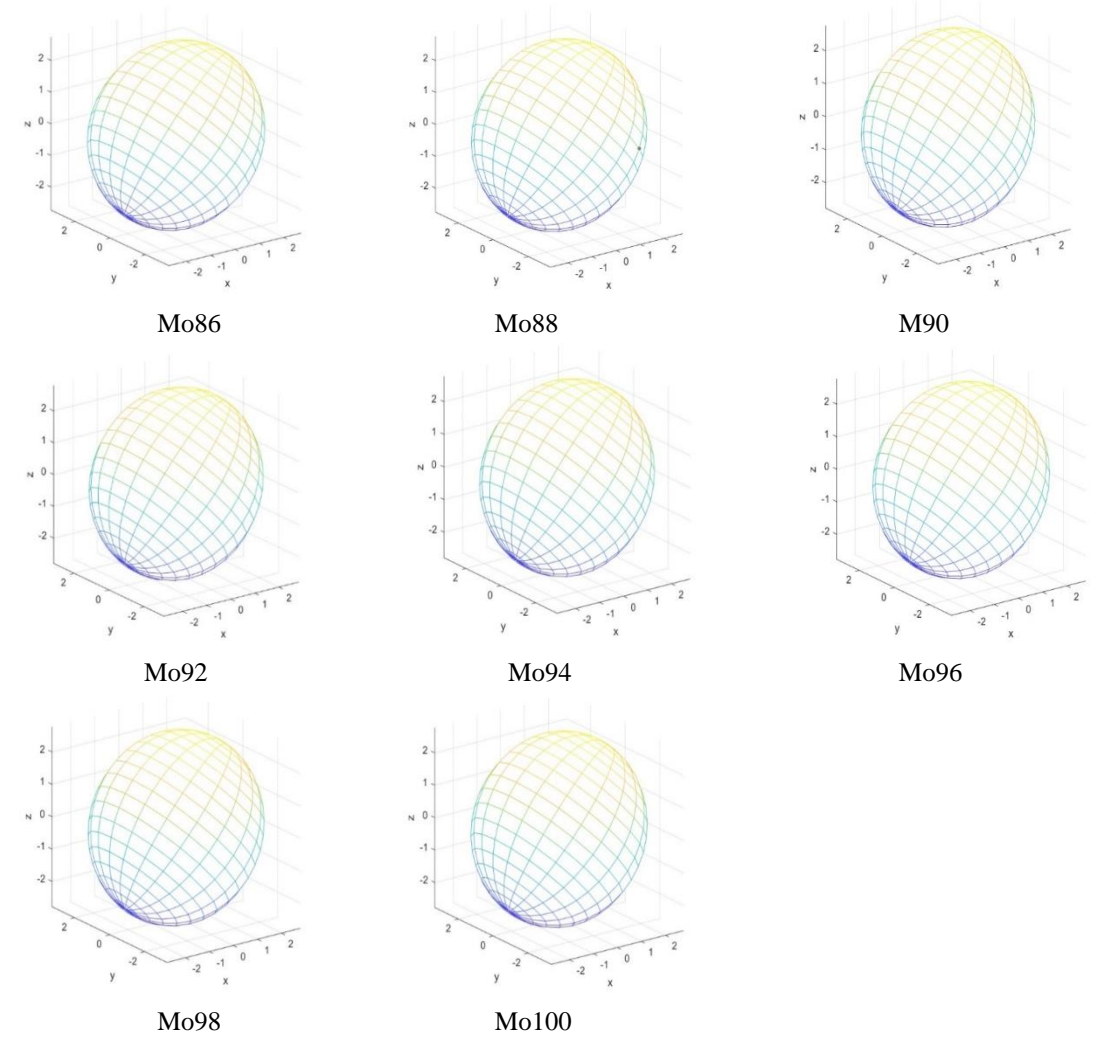


Figure 6. Three-dimensional shapes of the axially symmetric tetragon, deformation of the molybdenum ₄₂Mo isotope along the major (a) and minor (b) axis

4. Discussion

This study examined the nuclear structure of even-even molybdenum isotopes with mass numbers ranging from 86 to 100, focusing on the evaluation of parameters associated with nuclear deformation. The results revealed consistent trends in the behavior of the nuclei, with a gradual decrease in both the deformation parameters (β_2 , δ) and the electric quadrupole moment (Q_0) as the mass number increased. These changes indicate an increase in nuclear stability, particularly near magic neutron numbers such as N=50, where deformation values decreased significantly.

The decrease in deformation is also supported by a decrease in the electrical transition probabilities $B(E2)\uparrow$, as low values of these probabilities indicate a more spherical and less bulky nuclear shape. These results are consistent with the nuclear shell model, which predicts greater stability and less deformation in nuclei with full shells.

In addition, semi-major and semi-minor axes calculations revealed measurable differences between the isotopes, and the calculated root-square charge radii were in close agreement with experimental data. This agreement enhances the effectiveness of the theoretical models used, particularly the distorted shell model and the mathematical equations implemented using MATLAB.

Overall, the results confirm the power of theoretical models in predicting the structural evolution of isotopes and provide a deeper understanding of the relationship between nuclear distortion, shape, and stability in the intermediate mass region.

5. Conclusion

Nuclear structure analyses of molybdenum isotopes in the mass range from 86 to 100 have revealed regular trends in the fundamental nuclear parameters. Thus, the decrease in distortion coefficients and the probability of electrical transition with increasing mass number A indicates a systematic structural evolution among these isotopes. These results are in good agreement with theoretical predictions and experimental data, demonstrating the reliability of the computational methods used.

The results also highlight the particular stability of isotopes close to magic numbers, such as mass number 50, where distortion decreases significantly. Furthermore, the correlation between electric quadrupole moments, charge radii, and mass numbers supports our understanding of the dynamics of nuclear shape.

Overall, this study provides a clear insight into the behavior of molybdenum isotopes and contributes to a deeper understanding of nuclear distortion, transition probabilities, and charge distribution. The agreement between the calculated and experimental values enhances the credibility of the models applied in this research.

Acknowledgment

First and foremost, I extend grateful to other scholars whose work significantly informed this study, particularly Raman S., Nestor C.W., and Tikkanen G.R., along with additional valuable resources referenced in IHJPAS 37(4), 2025, page 221. Moreover, I would like to express my sincere gratitude to the College of Education for Pure Sciences – Ibn Al-Haytham for being the cornerstone of my academic journey and for facilitating the publication process of this research in a seamless and supportive manner.

Conflict of Interest

The authors declare that they have no conflicts of interest.

Funding

None.

Ethical Clearance

This study did not involve any human or animal experiments. All procedures and data analyses were conducted in accordance with the institution's ethical standards and applicable national regulations.

References

- 1. Boboshin I, Ishkhanov B, Komarov S, Orlin V, Peskov N, Varlamov V. Investigation of Quadrupole Deformation of Nucleus and its Surface Dynamic Vibrations. Int Conf Nucl Data Sci Technol. 2007;23:65-68.
- 2. Ali AH, Taha Idrees M. Study of deformation parameters (β2, δ) for 18, 20, 22, 24, 26, 28Ne isotopes in sdpf shell. Karbala Int J Mod Sci. 2020;6(1):78-82. https://doi.org/10.33640/2405-609X.1376.
- 3. Salim DA, Ebrahiem SA. Study of nuclear properties for the carbon (C) and oxygen (O) isotopes: Deformation parameters and root mean square radii. In: AIP Conf Proc. AIP Publishing; 2022. https://doi.org/10.1063/5.0093768.
- 4. Hassan IM, Ebrahiem SA, Al-Khafaji RSA. Calculated the quadrupole electrical transition |M(E2)|² Wu ↓ for even-even nuclides of strontium (78-100Sr and 66-76Ge). In: AIP Conf Proc. AIP Publishing; 2022. https://doi.org/10.1063/5.0094215.
- 5. Kumar R, Bhuyan M, Jain D, Carlson BV. Theoretical Description of Low-Energy Nuclear Fusion. In: Nuclear Structure Phys. CRC Press; 2020. p. 121–144.
- 6. Majeed FA, Obaid SM. Nuclear structure study of 22, 24Ne and 24Mg nuclei. Rev Mex Fis. 2019;65(2):159-167. https://doi.org/10.31349/revmexfis.65.159.
- 7. Hosseinnezhad A, Sabri H, Seidi M. The correlation of quadrupole transition rates of deformed nuclei by non-parametric approach. Nucl Phys A. 2022;1022:122431. https://doi.org/10.1016/j.nuclphysa.2022.122431.
- 8. Ali AH, Hassoon SO, Tafash HT. Calculations of Quadrupole Deformation Parameters for Nuclei in fp shell. In: J Phys Conf Ser. IOP Publishing; 2019. p. 012010. https://doi.org/10.1088/1742-6596/1178/1/012010.
- 9. Al-Sayed A, Abul-Magd AY. Level statistics of deformed even-even nuclei. Phys Rev. 2006;74(3):037301.
- 10. Yoshida K. Suddenly shortened half-lives beyond Ni-78: N = 50 magic number and high-energy nonunique first-forbidden transitions. Phys Rev C. 2019;100(2):024316. https://doi.org/10.1103/PhysRevC.100.024316.
- 11.Raheem EM, Hasan AAA, Alwan IH. Study of ground state properties of some Ni-isotopes using Skyrme-Hartree-Fock method. Iraqi J Phys. 2019;17(42):1-12. https://doi.org/10.20723/ijp.17.42.1-12.
- 12. Yoshida K. Suddenly shortened half-lives beyond Ni-78: N = 50 magic number and high-energy nonunique first-forbidden transitions. Phys Rev C. 2019;100(2):024316. https://doi.org/10.1103/PhysRevC.100.024316.
- 13. Heyde KLG. The nuclear shell model. Springer; 1994.
- 14.Ebrahiem SA, Zghaier HA. Estimation of geometrical shapes of mass-formed nuclei (A = 102-178) from the calculation of deformation parameters for two elements (Sn & Yb). In: J Phys Conf Ser. IOP Publishing; 2018. p. 012095. https://doi.org/10.1088/1742-6596/1003/1/012095.
- 15.Zghaier HA, Ebrahiem SA, Abdul-Jabbar H. Study the shapes of nuclei for heavy elements with mass number equal to $(226 \le A \le 252)$ through determination of deformation parameters for two elements (U & Cf). Ibn Al-Haitham J Pure Appl Sci. 2018;31(3):10-19. https://doi.org/10.30526/31.3.2022.

- 16.Hameed BS, Rejah BK. Study the nuclear structure of some cobalt isotopes. Baghdad Sci J. 2022;19(6 Suppl):1566. https://doi.org/10.21123/bsj.2022.7537.
- 17.Ma C, Zong YY, Zhao YM, Arima A. Evaluation of nuclear charge radii based on nuclear radii changes. Phys Rev C. 2021;104(1):014303. https://doi.org/10.1103/PhysRevC.104.014303.
- 18. Adamu A. A new measurement of nuclear radius from the study of β^+ -decay energy of finite-sized nuclei. J Rad Nucl Appl. 2021;6(1):45. https://doi.org/10.18576/jrna/060107.
- 19.Mahmood PF. Ground state properties of even-even 30–92Ca isotopes using HFB theory. Kirkuk J Sci. 2024;19(1):43–50. https://doi.org/10.32894/kujss.2024.146573.1136.
- 20.Pritychenko B, Birch M, Singh B. Revisiting Grodzins systematics of B(E2) values. Nucl Phys A. 2017;962:73–102. https://doi.org/10.1016/j.nuclphysa.2017.03.011.
- 21. Akkoyun ST, Bayram A, Kara SO. A study on estimation of electric quadrupole transition probability in nuclei. J Nucl Sci. 2015;2(1):7–10.
- 22.Bonatsos D. Interacting boson models of nuclear structure. In: Hodgson PE, editor. Oxford Univ Press; New York: 1988. p. 1–264.
- 23. Angeli I, Marinova KP. Table of experimental nuclear ground state charge radii: An update. At Data Nucl Data Tables. 2013;99(1):69–95. https://doi.org/10.1016/j.adt.2011.12.006.
- 24. Taha H, Jiang ZT, Henry DJ, Amri A, Yin CY, Alias AB, et al. Improved mechanical properties of sol-gel derived ITO thin films via Ag doping. Mater Today Commun. 2018;14:210–24. https://doi.org/10.1016/j.apsusc.2020.147164.
- 25.Pritychenko B, Birch M, Singh B, Horoi M. Tables of E2 transition probabilities from the first 2⁺ states in even-even nuclei. At Data Nucl Data Tables. 2016;107:1–139. https://doi.org/10.1016/j.adt.2015.10.001.
- 26.Pritychenko B, Birch M, Horoi M, Singh B. B(E2) evaluation for $0^+ \rightarrow 2^+$ transitions in even-even nuclei. arXiv. 2013 Feb 27. Available from: https://doi.org/10.1016/j.nds.2014.07.021.
- 27. Krane KS. Introductory nuclear physics. John Wiley & Sons; 1991. p. 231.
- 28.Bao S, Li K, Ning P, Peng J, Jin X, Tang L. Highly effective removal of mercury and lead ions from wastewater by mercaptoamine-functionalised silica-coated magnetic nano-adsorbents: behaviours and mechanisms. Appl Surf Sci. 2017;393:457–66. https://doi.org/10.1016/j.apsusc.2016.09.098.
- 29.Raman S, Nestor CW, Tikkanen P. Transition probability from the ground to the first-excited 2⁺ state of even-even nuclides. At Data Nucl Data Tables. 2001;78(1):1–128. https://doi.org/10.1006/adnd.2001.0858.
- 30.Angeli I, Marinova KP. Table of experimental nuclear ground state charge radii: An update. At Data Nucl Data Tables. 2013;99(1):69–95. https://doi.org/10.1016/j.adt.2011.12.006.